ATOMISTIC STUDIES OF PROPERTIES OF HELIUM IN BCC IRON USING THE NEW HE–FE POTENTIAL—David M. Stewart, Stanislav Golubov (Oak Ridge National Laboratory and the University of Tennessee), Yuri Ostesky, Roger E. Stoller, Tatiana Seletskaia, and Paul Kamenski (Oak Ridge National Laboratory)

OBJECTIVE

The objective of this work is to use molecular dynamics techniques to increase understanding of the behavior of transmutation-produced helium in reduced-activation ferritic/martensitic steels that are candidate materials for fusion reactors. As there is no suitable iron-carbon-helium interatomic potential, simulations are performed using helium in pure iron.

SUMMARY

We have performed atomistic simulations of helium behavior in iron using a new 3-body Fe–He inter-atomic potential combined with the Ackland iron potential. With the ORNL potential, interstitial helium is very mobile and coalesces to form interstitial clusters. If the He cluster is sufficiently large the cluster can push out an Fe interstitial, creating a Frenkel pair. The resulting helium–vacancy cluster is not mobile. The ejected SIA is mobile, but is weakly trapped by the He–V cluster. If more helium atoms join the He–V cluster, more Fe interstitials can be pushed out, and they combine to form an interstitial dislocation loop. In the reverse process, multiple helium atoms can be trapped in a single vacancy, and if there are few enough, the vacancy can recombine with an Fe interstitial to create a helium interstitial cluster. These mechanisms are investigated together in larger simulations that examine the nucleation of He defects. Helium bubbles of sizes 1–6 nm are also studied. In order to estimate the amount of helium present from an observed bubble size distribution, it is necessary to understand the relationships between bubble size, pressure and helium content. Extensive atomistic simulations of such bubbles are compared to show effect of temperature, interatomic potentials used and helium concentration.

PROGRESS AND STATUS

Introduction

Helium produced in neutron irradiated iron affects the mechanical properties. Predicting the growth, migration and coalescence behavior of helium bubbles is very sensitive to the assumed properties of individual He interstitials and helium-vacancy clusters [1]. A new He–Fe inter-atomic potential has been developed at ORNL, based on extensive fitting to first-principles calculations of point defects and clusters [2–4]. This potential has been used to investigate the properties of helium, helium-vacancy clusters and helium bubbles in MD and MS simulations.

Helium diffuses very fast in the matrix, but is easily trapped in vacancies [5]. It is possible for a self-interstitial to recombine with the vacancy, knocking the helium back into an interstitial position. Previous calculations [6] showed that recombination is possible not only for a single substitutional He, but even when the vacancy contains multiple Helium atoms.

Previous calculations [6] also showed that the reverse process (i.e. Frenkel pair formation) can happen—an iron atom is pushed out of its lattice site, creating a He–V cluster and an SIA. As more helium joins the cluster, more Frenkel pairs are formed, creating larger defects. The He–V defects nucleated in this manner are nascent bubbles. Helium bubbles are more stable than voids and continue to grow as more helium and vacancies diffuse to the bubble.

Simulation Method

The general procedure followed is: Generate perfect BCC lattice. Introduce the defect(s) to be studied. Relax at constant volume using a mixture of conjugate gradient and simulated annealing, and save the atom positions in units of the lattice constant. Start the MD simulation.

The MD simulations used NVE (constant **n**umber of atoms, constant **v**olume and constant **e**nergy) dynamics. The lattice constant and initial velocities were chosen to give close to zero pressure and the desired initial temperature. The boundary conditions are periodic in *X*, *Y* and *Z*, which are ⟨100⟩ directions. The velocity Verlet algorithm with a timestep of 0.3fs is used. As volume and temperature correction are not used, when processes that release energy are simulated the temperature and pressure both rise during the simulation.

Coalescence

Previous He coalescence simulations [6–8] were run at two different concentrations: 125 helium atoms in a 31×31×31 BCC iron matrix (60,000 iron atoms) and 125 helium atoms in a 40×40×40 BCC iron matrix (128,000 iron atoms). These give concentrations of 2089 and 976 appm He respectively. New, much larger simulations have now been run at two concentrations: 1000 and 500 helium atoms in a 80×80×80 BCC iron matrix (1,024,000 iron atoms). These give concentrations of 976 and 488 appm He respectively. For all four simulations, the concentration of vacancies created is plotted as a function of time in Figure 1.

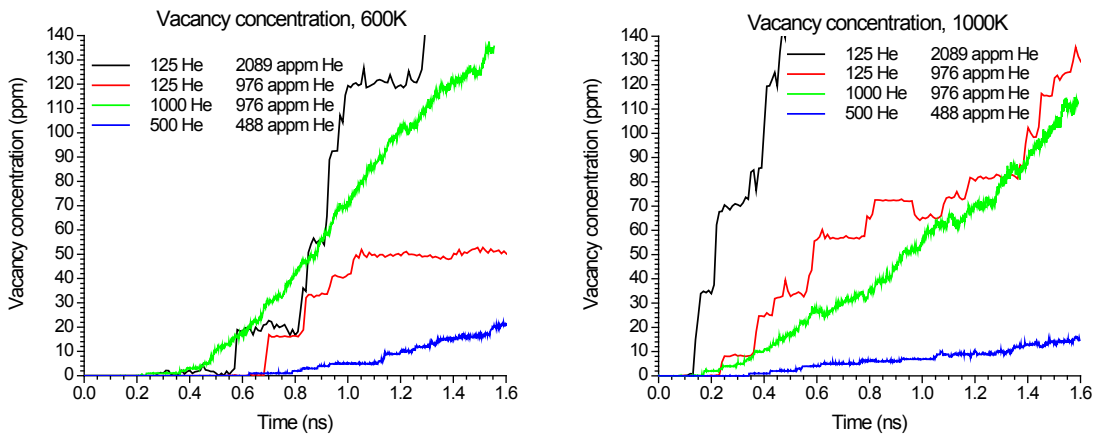

Figure 1. Coalescence for different concentrations at (a) 600 K and (b) 1000 K.

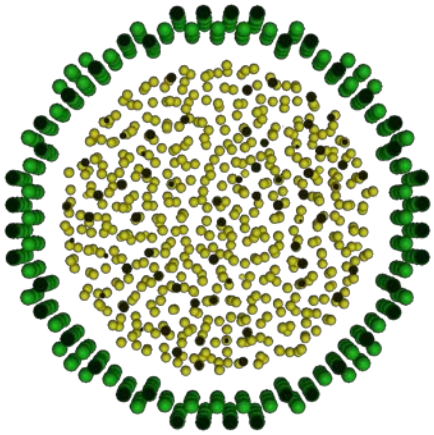

Figure 2. 4 nm 0.5 He/V bubble at 100 K.

Helium bubbles

The He–V defects nucleated in the coalescence simulation are nascent bubbles. We have also simulated larger ones. Bubbles of diameters of 1, 1.5, 2, 4 and 6 nm were investigated. They consist of helium atoms in a spherical void containing 59, 169, 339, 2741 or 9577 vacancies

respectively. Figure 2 shows a cross-section of a 4 nm (2741 vacancy) bubble with a helium to vacancy ratio of one half.

In a void, the surface matrix atoms move inwards slightly. For a helium bubble, the pressure from the helium pushes them back outwards again. We define a bubble as under-pressurized, equilibrium or over-pressurized, if the net effect is to move the matrix atoms inwards, stationary or outwards respectively.

The equilibrium He/V ratio (i.e. the ratio that results in no dilation [7]) is calculated for bubbles of different sizes and temperatures and plotted in Figure 3. The plots show that the ratio decreases with temperature, and larger bubbles show a stronger temperature variation. This is expected as the helium is liquid (as will be shown in a later section) and has a larger coefficient of thermal expansion than iron.

The plots also show that the equilibrium ratio as a function of size has a peak. The size where the peak occurs is temperature dependant, decreasing with increasing temperature. For all but very low temperatures the peak is near 1.5 nm. Above peak size, the equilibrium ratio decreases with size because the pressure goes as $2\gamma/r$. Below peak size, the equilibrium ratio decreases with size because the space available for helium decreases rapidly due to the increasing fraction of the volume accounted for by the He-free gap.

Trinkaus [9] classified He–V clusters and bubbles into three size categories: bubble nuclei, non-ideal gas bubbles and ideal gas bubbles. The boundary between bubble nuclei and non-ideal gas bubbles is given as a diameter of 2 nm, close to the size where we observe the peak equilibrium ratio.

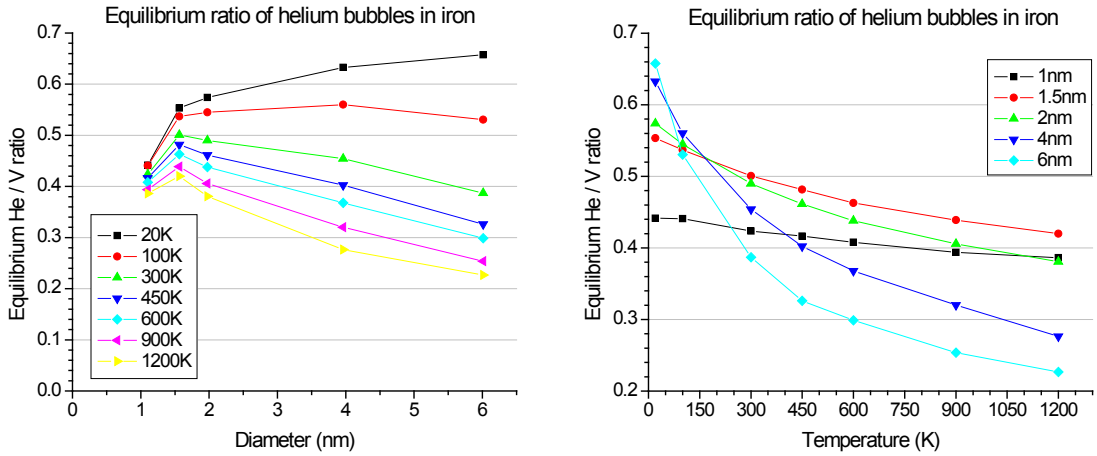

Figure 3. Equilibrium He/V ratio as a function of a) bubble size and b) temperature.

We have performed simulations of helium bubbles using different combinations of Fe–He and He–He potentials. Fe–He potentials used are ORNL [2–4], Juslin–Nordlund [10] and Wilson [11]. He–He potentials used are Aziz [12], Beck [13] and Wilson [11]. All calculations used the Ackland Fe–Fe potential [14].

Figure 4 shows dilation of a bubble as a function of He/V ratio for different temperatures. The graph on the left uses the ORNL potential with the Aziz potential and the graph on the right uses the Wilson potential. With the Wilson potential the curves cross the zero (equilibrium) line at a significantly larger (15–25% higher) He/V ratio at all temperatures, and also show a larger spread with temperature.

Figure 5 shows equilibrium ratios calculated using five different combinations of potentials. The results fall into two groups, one consisting of ORNL+Aziz and ORNL+Beck, and the other consisting of JN+Aziz, Wilson and Wilson+Aziz.

The choice of helium–helium inter-atomic potential did not significantly affect helium bubble equilibrium ratio results. The Wilson and Juslin–Nordlund iron–helium potentials both produced the same equilibrium ratios. Results from the ORNL potential are significantly different than the other Fe–He potentials. With the ORNL potential the bubble has a larger gap, leading to lower He/V ratios at a given size and temperature.

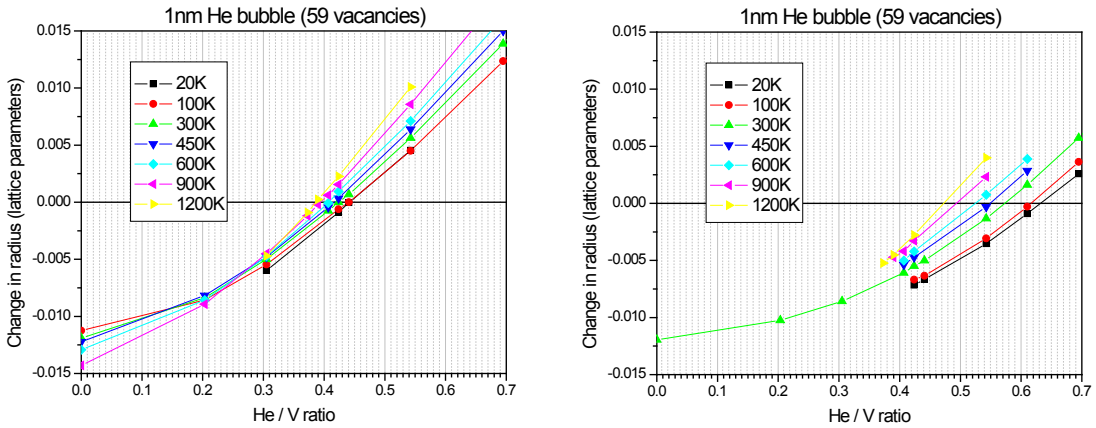

Figure 4. Dilation of 1 nm bubble. (a) Ackland97+ORNL+Aziz. (b) Ackland97+Wilson

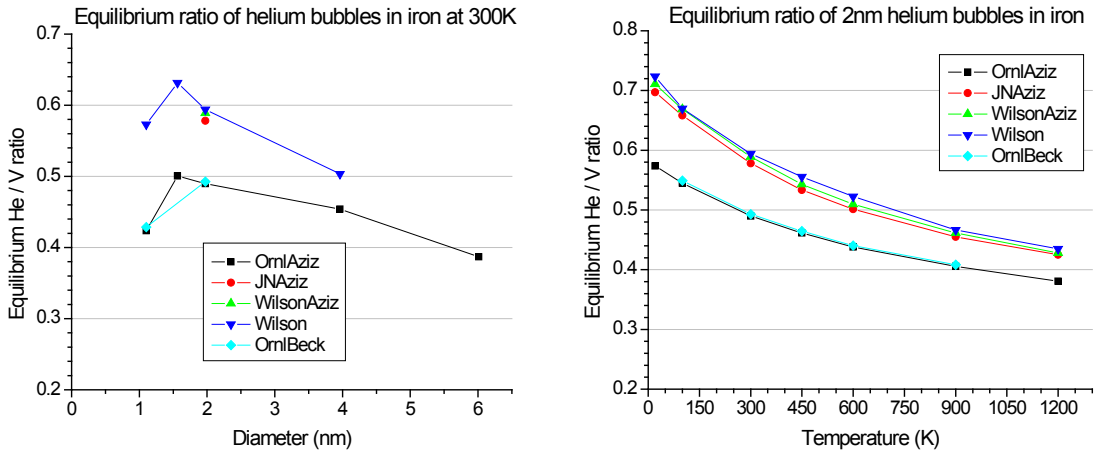

Figure 5. Equilibrium He/ V ratio as a function of a) size and b) temperature for different potentials

The pressure of the helium bubble is fit to three theoretical models for the equation of state of a gas and shown in Figure 6. The ideal gas law and the Van der Waals equation do not fit. The hard sphere equation of state [15] fit to bubbles 1.5 nm diameter and above, i.e. the size that Trinkaus [9] classes as non-ideal gas bubbles.

The pressure is calculated as Virial per unit volume. However, since the bubble contains a gap between the iron and the helium, there are two different volumes to consider. The graph on the left is calculated using only the volume actually occupied by helium. The graph on the right is calculated using the volume of the bubble, including the gap.

Also included on the graphs is the Laplace pressure, i.e. the pressure expected from surface energy considerations. This is calculated in two ways also; using the facet-averaged standard iron surface energy density value for iron of 1.82 J/m^2 and using molecular static calculations to determine the surface energy of the bubble size in question.

The hard sphere equation of state has one parameter, the diameter *d* of the hard spheres. At 300 K, The helium volume calculation fit with *d* = 0.2017 nm, and bubble volume calculation fit with *d* = 0.259 nm. At 600 K, The helium volume calculation fit with *d* = 0.193 nm, and bubble volume calculation fit with *d* = 0.244 nm.

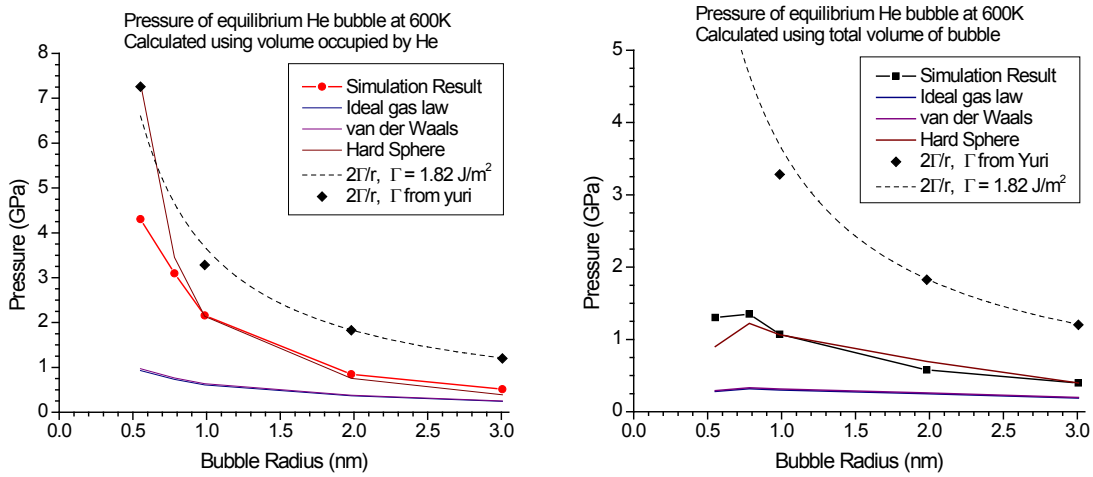

Figure 6. Pressure of He bubble fit to equations of state and surface energy.

The trajectory decomposition method described in [8] and [16] was used to calculate the diffusion coefficient of the helium atoms in a bubble. As the helium atoms cannot escape the bubble, the time segments cannot be too long or the diffusion coefficient will be underestimated. Here we decomposed the atom trajectory into segments of up to 15 ps. For each segment size, the average of the diffusion coefficients of each segment is calculated. This calculation is done for segment sizes of 7.5ps to 15 ps in increments of 0.3 ps, and the average of these is calculated. This is then repeated for 100 (or all, if less than 100) atoms in the bubble and the final value is the average of these atoms.

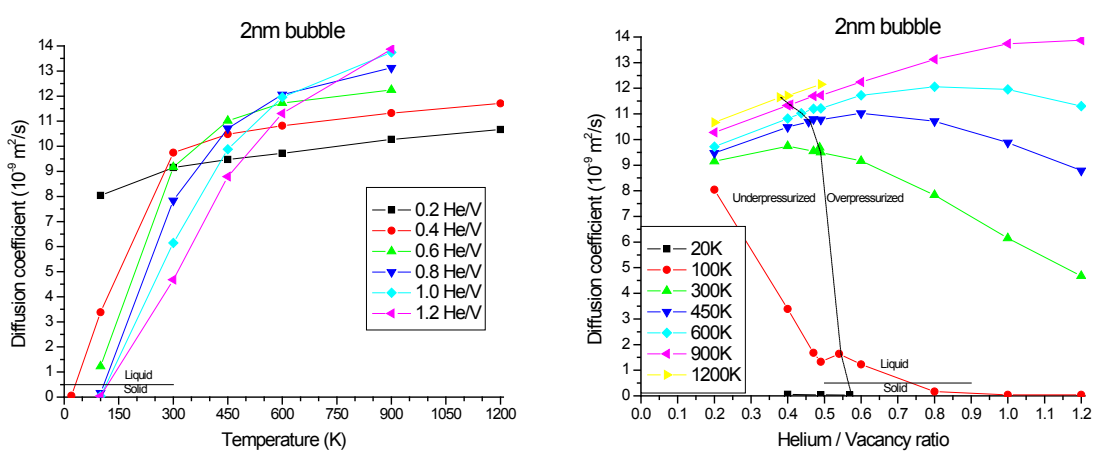

Figure 7. Diffusion coefficient of He atoms in bubble shows state.

The results are plotted in Figure 7. A diffusion coefficient near or below 0.5×10^{-9} m^2/s indicates that the helium in the bubble is solid [17]. The graphs show that most of the bubbles studied are liquid; solid helium only occurs in bubbles at very low temperatures or very high He/V ratios.

The diffusion coefficient increases with temperature as expected, but saturates at high temperatures. This saturation is likely due to the confinement of the atom within the bubble, i.e. it is an artifact of the choice of segment lengths to study. A shorter time segment would have been better for these high temperatures but not as good for lower temperatures.

The D vs. ratio plot includes the equilibrium ratios, dividing the space into areas representing underpressurized and overpressurized bubbles.

References

[1] S.I. Golubov, R.E. Stoller, S.J. Zinkle, and A.M. Ovcharenko, Kinetics of coarsening of helium bubbles during implantation and post-implantation annealing, Journal of Nuclear Materials 361 (2007), pp. 149–159.

[2] T. Seletskaia, Y.N. Osetsky, R.E. Stoller, and G.M. Stocks, Magnetic Interactions Influence the Properties of Helium Defects in Iron, Physical Review Letters 94 (2005), pp. 046403.

[3] T. Seletskaia, Y.N. Osetsky, R.E. Stoller, and G.M. Stocks, Calculation of helium defect clustering properties in iron using a multi-scale approach, Journal of Nuclear Materials 351 (2006), pp. 109–118.

[4] T. Seletskaia, Y.N. Osetsky, R.E. Stoller, and G.M. Stocks, Development of a Fe He interatomic potential based on electronic structure calculations, Journal of Nuclear Materials 367 (2007), pp. 355–360.

[5] H. Trinkaus and B. Singh, Helium accumulation in metals during irradiation–where do we stand? Journal of Nuclear Materials 323 (2003), pp. 229–242.

[6] D.M. Stewart, July 2009 semiannual report.

[7] David M. Stewart, Yuri N. Osetsky and Roger E. Stoller, Atomistic studies of formation and diffusion of helium clusters and bubbles in BCC iron, Accepted for publication in Journal of Nuclear Materials

[8] David M. Stewart, Yuri N. Osetsky, Roger E. Stoller, Stanislav I. Golubov, Tatiana Seletskaia and Paul J. Kamenski, Atomistic studies of helium defect properties in bcc iron: comparison of He–Fe potentials, Philosophical Magazine, Volume 90, Issue 7 & 8 (March 2010) pp. 935 – 944

[9] H. Trinkaus, Energetics and formation kinetics of helium bubbles in metals, Radiation Effects, 78 (1983) pp. 189-211

[10] K. Nordlund and S. Dudarev, Interatomic potentials for simulating radiation damage effects in metals, Comptes rendus-Physique (2008).

[11] W. Wilson and R. Johnson, Rare Gases in Metals, Interatomic Potentials and Simulation of Lattice Defects, Battelle Institute Materials Science Colloquia, 1972, 375-390 (1972).

[12] R. Aziz, A. Janzen, and M. Moldover, *Ab Initio* Calculations for Helium: A Standard for Transport Property Measurements, Phys. Rev. Lett. 74 (1995), pp. 1586–1589.

[13] D.E. Beck, A new interatomic potential function for helium, Mol. Phys., 14 (1968) 311-315

[14] G.J. Ackland, D.J. Bacon, A.F. Calder, and T. Harry, Computer simulation of point defect properties in dilute Fe-Cu alloy using a many-body interatomic potential, Philosophical Magazine A-Physics of Condensed Matter Structure Defects and Mechanical Properties 75 (1997), pp. 713–732.

[15] I.R. Brearley and D.A. MacInnes, An improved equation of state for inert gases at high pressures, Journal of Nuclear Materials 95 (1980) pp. 239-252

[16] Yuri N. Osetsky, Atomistic Study of Diffusional Mass Transport in Metals, Defect and Diffusion Forum 188 – 190 (2001) pp. 71-92

[17] S. M. Hafez Haghighat, G. Lucas and R. Schäublin, State of a pressurized helium bubble in iron, Europhysics Letters, 85 (2009) 60008